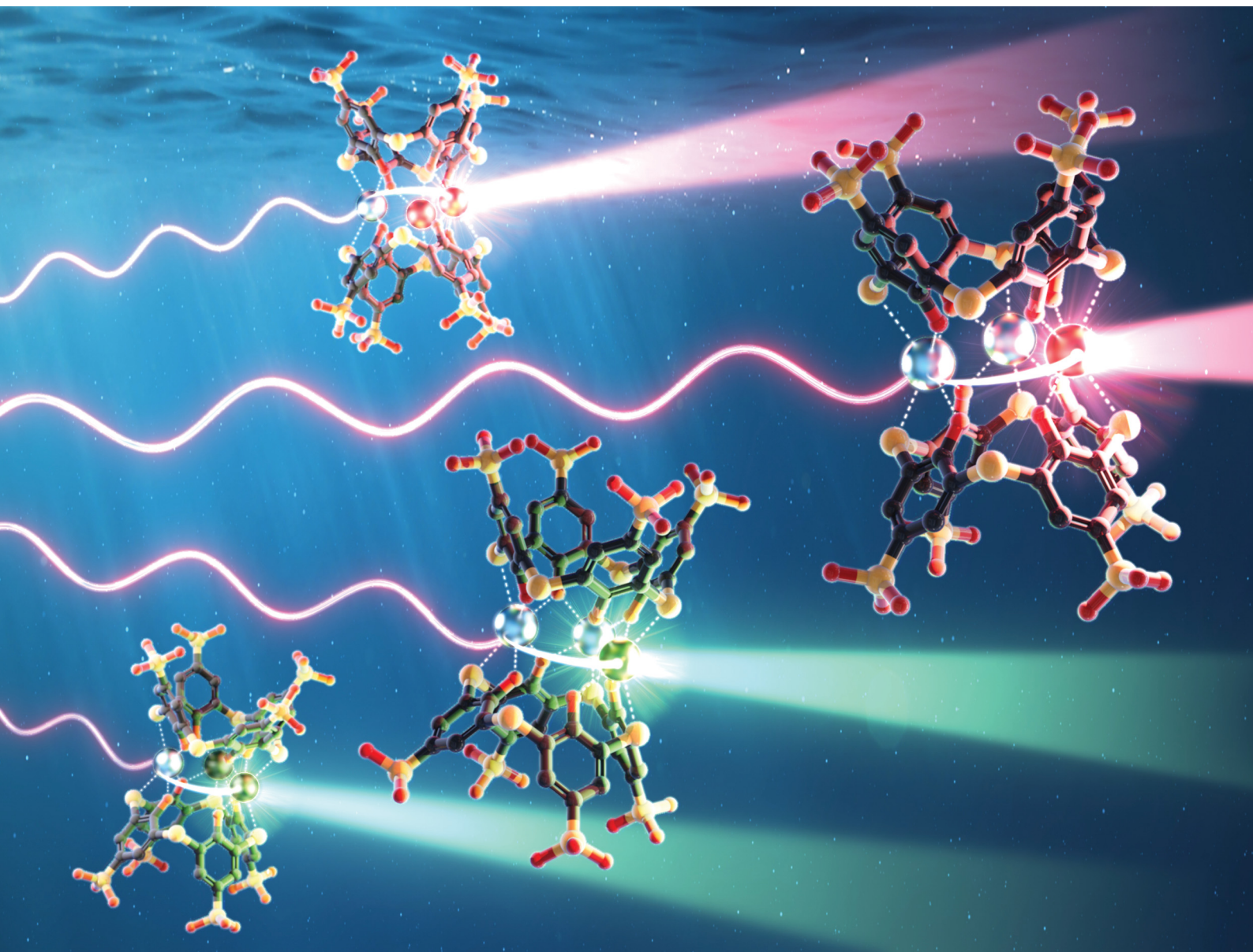# ChemComm

Chemical Communications

ROYAL SOCIETY
OF CHEMISTRY

COMMUNICATION
Ryunosuke Karashimada, Nobuhiko Iki *et al.*
Heterotrilantanide cluster complexes exhibiting
up-conversion luminescence in water

Check for updates

Heterotrilantanide cluster complexes exhibiting up-conversion luminescence in water†

Ryunosuke Karashimada, [ID]* Koki Musha and Nobuhiko Iki [ID]*

Heterotrinuclear cluster complexes consisting of Er–Yb- and Tb–Yb–thiacalix[4]arene-*p*-tetrasulfonate exhibited photon up-conversion luminescence in water, in which visible light emission from the Er and Tb center, respectively, was induced by two-photon excitation of the Yb center with near-infrared light.

Photon up-conversion (UC) is a fascinating optical phenomenon in which low-energy (long-wavelength) photons are converted to high-energy (short-wavelength) photons. This is one of the non-linear optical phenomena consisting of several types of optical processes, such as two-photon absorption, second harmonic generation, excited-state absorption, energy transfer UC, cooperative energy transfer, and triplet–triplet annihilation.[1–8] The advantageous features of photon UC can be applied, for instance, to the bio-imaging of deep tissues using near-infrared (NIR) light as the excitation source or to widen the sensitivity and efficiency of silicon-type solar cells near the NIR region.[9–11] The lanthanide (Ln)-doped system, such as metal–organic frameworks (MOFs) or inorganic materials (oxides and fluorides), have been reported in many UC systems which have the advantage of an easy synthesis of the materials by doping the Ln pair and reducing the deactivation process derived from the host structure. However, these materials have limited energy-transfer efficiencies because different Ln ions are randomly distributed in the host materials. Furthermore, when used as bio-imaging probes, UC materials need to be nanosized.

Metal complexes, which have more than two metal centers comprising the same Ln ions, different Ln ions, or Ln-d-block transition metal ions, have the potential for molecular UC. These complexes have the advantage of molecular size and designability to rigorously control the distance between metal ions for effective energy transfer.[4,12–15] Although metal complex

Graduate School of Environmental Studies, Tohoku University, 6-6-07,
Aramaki-Aoba, Aoba-ku, Sendai 980-8579, Japan.
E-mail: karashimada@tohoku.ac.jp, iki@tohoku.ac.jp

† Electronic supplementary information (ESI) available: Experimental, estimation of the Yb-centered luminescence intensity, Figs. S1-S9, and Tables S1-S3. See: https://doi.org/10.1039/d4cc06573e
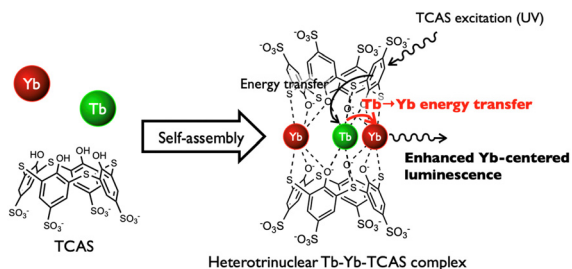
systems have the above-mentioned benefits, severe problems remain with achieving molecular UC because the efficiency of UC luminescence is significantly affected by deactivation of X–H (X = C, O, N) vibration in the ligand. Moreover, in aqueous systems such as bodily fluids and biotissues, the excited states of the Ln centers are readily quenched by the O–H oscillator of the surrounding water. Despite these difficulties, only a few molecular UC systems have been recently reported. For example, Charbonniére and co-workers have reported molecular UC luminescence in an aqueous solution (H_2O or D_2O) by dimerization of mononuclear Ln complexes using F^- or hetero Ln ions and a polynuclear Ln complex based on phosphonated macrocyclic or pyridyl-type ligands at room temperature.[16–19] Piguet *et al.* have also reported molecular UC systems, such as a mononuclear complex and a Ln-transition metal-type heteronuclear complex system based on helical-type ligands, at extremely low or room temperature in a solid state or an organic solvent.[20–26] Additionally, the mononuclear Er complex with NIR absorption ligand resulted in UC luminescence by ligand-to-Er energy transfer.[27] In other cases, some molecular cluster-aggregation systems can exhibit molecular UC in CD_3OD.[28–30] According to these reports, the design of metal complexes to achieve UC luminescence is important to shorten the distance between metal ions for effective energy transfer and to eliminate deactivation processes, such as X–H (X = C, O, N) vibration. Therefore, precise design of the complex or system is crucial for achieving molecular UC luminescence. A promising candidate, in particular, is a complex with Ln–Ln′ clusters, in which Ln ions are separated only by a coordination atom.

We have previously reported that thiacalix[4]arene-*p*-tetrasulfonate (TCAS, Fig. 1) can form cluster-type homotrinuclear complexes (Ln_3TCAS_2) and heterotrinuclear complexes ($Ln_{3-x}Ln'_xTCAS_2$, x = 1, 2) with Ln ions by simply mixing the components (Fig. 1).[31–36] In the cluster complex, three Ln ions are arranged in the form of a right-angled isosceles triangle. Since the Ln ions are in close proximity, 3.75 and 4.57 Å in the Gd_3TCAS_2 complex,[32,37] energy transfer efficiency by dipole–dipole interaction between Ln and Ln′ in the heterotrinuclear

Fig. 1 Formation of the heterotrinuclear Tb–Yb–TCAS complex *via* self-assembly and enhancement of Yb-centered luminescence through TCAS to Tb → Yb energy transfer.
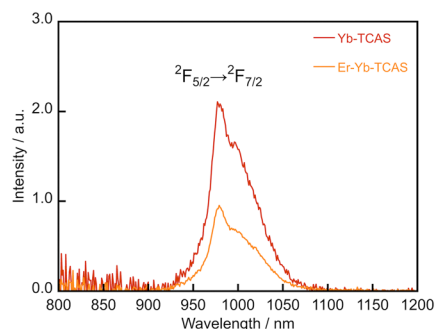

Fig. 2 Emission spectra of the Yb–TCAS (red) and Er–Yb–TCAS (orange) systems. λ_{ex} = 313 nm, Yb–TCAS system: [Yb] = 2.5 μM, [TCAS] = 5.0 μM, [HEPES] = 10 mM, pH 7.4. Er–Yb–TCAS system: [Er] = [Yb] = 2.5 μM, [TCAS] = 5.0 μM, [HEPES] = 10 mM, pH 7.4.

complex should be sufficiently high. In fact, the Tb–Yb heterotrinuclear complex showed enhanced Yb-centered luminescence *via* Tb → Yb energy transfer, with an efficiency of 45% (Fig. 1).[34,35] By virtue of cluster formation, the TCAS is a suitable ligand for achieving energy transfer between Ln ions. Therefore, UC luminescence is expected from the direct excitation of Ln ions and the energy transferred to different Ln′ ions.

Motivated by the above investigation, herein we report our challenge to observe UC luminescence in a new heteronuclear system, the Er–Yb–TCAS, in which the Er–Yb pair is reported to emit visible UC luminescence from the Er center by NIR excitation of the Yb center.[1,38,39] Furthermore, the UC of the Tb–Yb–TCAS system will also be investigated using Yb excitation.[1,18,19,28]

Firstly, we confirmed the formation of the heterotrinuclear complex, $Er_{3-x}Yb_xTCAS_2$ (x = 1, 2). In the HPLC measurement, the chromatogram of the mixture of Er, Yb, and TCAS solution (Er–Yb–TCAS system) showed a single peak, the retention factor of which was the same as the Ln_3TCAS_2 complex (Fig. S1, ESI†). The Er–Yb–TCAS system was further investigated by ESI-MS measurement, which showed an isotopic distribution corresponding to the homo- and heterotrinuclear $Er_{3-x}Yb_xTCAS_2$ (x = 0–3) complexes (Fig. S2–S5 and Tables S1–S3, ESI†). These results revealed that the mixture of Er, Yb, and TCAS forms a mixture of homo- and heterotrinuclear $Er_{3-x}Yb_xTCAS_2$ (x = 0–3) complexes, which is consistent with the previous studies.[32,34]

To evaluate the energy transfer between Er–Yb, we prepared two samples, Er–Yb–TCAS and Yb–TCAS systems. These samples consist of a completely formed Ln_3TCAS_2 complex and free TCAS because of containing excess amount of TCAS (Fig. S6, ESI†), which condition references to the previous study.[34] The Er–Yb–TCAS system showed NIR luminescence at 980 nm, corresponding to the emission band of Yb^{3+} ($^2F_{5/2} → ^2F_{5/2}$) upon excitation of the TCAS ligand at 313 nm (Fig. 2). The Yb-centered luminescence of the Er–Yb–TCAS system consists of not only heterotrinuclear complexes ($Er_{3-x}Yb_xTCAS_2$, x = 1, 2) but also concomitantly formed Yb_3TCAS_2; thus, the intensity at 980 nm is their sum. Meanwhile, a pure Yb_3TCAS_2 solution, termed as Yb–TCAS system, was also prepared using the same procedure for the Er–Yb–TCAS system, without the Er ion. The Yb–TCAS system showed Yb-centered luminescence at 980 nm owing to the homotrinuclear complex Yb_3TCAS_2. Notably, the intensity of the NIR luminescence of the Yb–TCAS system ($I_{Yb-TCAS}$ ≈ 2.08) was approximately 2.2 times higher than that of the Er–Yb–TCAS system ($I_{Er-Yb-TCAS}$ ≈ 0.93) in

the presence or absence of Er ions. Furthermore, based on the concentration of the Ln_3TCAS_2 complex, that of the Yb–TCAS system was approximately 7.6 times than that of the Er–Yb–TCAS system based on the concentration of Ln_3TCAS_2 complex (the detail see ESI†). This difference suggests a Yb → Er energy transfer in the heterotrinuclear complex ($Er_{3-x}Yb_xTCAS_2$, x = 1, 2), which results in weaker luminescence.

Luminescence lifetime analysis is a useful tool for investigating energy transfer mechanisms. The Yb-centered luminescence of Yb_3TCAS_2 showed a single exponential decay with a lifetime of τ = 0.33 μs (Fig. 3a). In contrast, the Er–Yb–TCAS system showed short- and long-lived components (0.011 and 0.30 μs, respectively) (Fig. 3b). As determined by the similarity to the τ value of Yb_3TCAS_2 luminescence, the longer component (τ = 0.30 μs) was attributed to the Yb_3TCAS_2 complex present in the sample solution. Hence, the shorter component (τ = 0.011 μs) can be attributed to the luminescence of the heterotrinuclear complexes ($Er_{3-x}Yb_xTCAS_2$, x = 1, 2). The shorter lifetime of the heterotrinuclear complex suggests the presence of a deactivation path through the Yb → Er energy transfer, which is consistent with the decrease in the Yb-centered luminescence in the Er–Yb–TCAS system.

The efficiency of the Yb → Er energy transfer, η, calculated using eqn (1) is extremely high (97%).

$$\eta = 1 - \tau/\tau_0 \qquad (1)$$

where τ_0 is the lifetime in the absence of the acceptor Er (0.33 μs) and τ is the lifetime in the presence of the acceptor
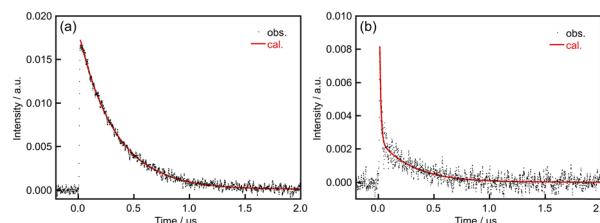

Fig. 3 Decay curves (black dots) and calculation curves (solid red line) of the (a) Yb–TCAS and (b) Er–Yb–TCAS systems. Yb–TCAS system: [Yb] = 30 μM, [TCAS] = 20 μM, [HEPES] = 10 mM, pH 7.4. Er–Yb–TCAS system: [Er] = [Yb] = 15 μM, [TCAS] = 20 μM, [HEPES] = 10 mM, pH 7.4, λ_{ex} = 337.1 nm.

(0.011 μs). The efficiency of Förster-type energy transfer depends on the distance between the donor and acceptor, with an inverse sixth power law owing to the dipole–dipole coupling mechanism. As mentioned earlier, the distances between the Ln ions in the Ln_3TCAS_2 complex are 3.75 and 4.57 Å.[32,37] The high efficiency of the Yb → Er energy transfer should be caused by the proximity of Ln ions in the cluster formation. Artizzu *et al.* reported the efficiency of the Yb → Er energy transfer to be 99.5% in an Er–Yb–Q complex (Q: 8-quinolinolate),[40,41] in which the Er−Yb distance was 3.5 Å. In comparison, the slightly longer Er–Yb distance in the Er–Yb–TCAS system may be responsible for the slightly lower energy transfer efficiency. Although there is a possibility that the signal at approximately 1550 nm was due to the $^4I_{13/2} \rightarrow {}^4I_{15/2}$ transition in the Er center, the Er_3TCAS_2 complex contained in the $Er_{3-x}Yb_xTCAS_2$ (x = 0–3) mixture did not show the signs of Er-centered luminescence in the spectra and decay curve, respectively (Fig. S7, ESI†). This may be caused by the efficient deactivation of the $^4I_{13/2}$ state by the coordinating water molecules with two O–H phonons,[42] and an inefficient excitation path through the TCAS center. Therefore, Er-centered luminescence was negligible in the analysis of the NIR signals.

Considering the high efficiency of energy transfer between Yb and Er ions in heterotrinuclear complexes, direct excitation of the Yb center with a strong excitation source may induce UC luminescence from the Er center. Using a high-power NIR laser (2.2 W, 972 nm) suitable for $^2F_{5/2} \leftarrow {}^2F_{7/2}$ excitation of Yb, UC luminescence was detected in the visible region at 548 and 663 nm from the heterotrinuclear complexes ($Er_{3-x}Yb_xTCAS_2$, x = 1, 2) (Fig. 4a). The emission bands could be assigned to Er-centered transitions ($^4S_{3/2} \rightarrow {}^4I_{15/2}$ and $^4F_{9/2} \rightarrow {}^4I_{15/2}$), suggesting that the UC luminescence originated from the Yb → Er energy transfer by Yb excitation. To confirm the UC characteristics, we investigated the dependence of the emission intensity on the excitation power using a log–log plot (Fig. 4c). The plot showed a linear relationship with a slope of 1.9, suggesting that the luminescence originates from the energy-transfer UC involving two photons (Fig. S8a, ESI†). Additionally, the $Er_{3-x}Yb_xTCAS_2$ (x = 0–3) complexes remained unchanged during NIR laser irradiation (Fig. S9a and b, ESI†). The UC luminescence by the heterotrinuclear complexes ($Er_{3-x}Yb_xTCAS_2$, x = 1, 2)

in water at room temperature is remarkable because these complexes have two or three coordinated water molecules in aqueous solution.[31] Although Ln ions are surrounded by many O–H oscillators as strong quenchers, the energy transfer is efficient owing to the close proximity of the Ln centers, which compete with the quenching path, resulting in UC luminescence. Previously reported molecular UC systems are self-assembled supramolecular edifices formed by either hydrogen bonding and π stacking interactions,[16] or an equilibrium mixture of heteronuclear complexes consisting of mononuclear complexes and free metal ions.[17–19] By contrast, our system is based on heterotrinuclear complexes ($Er_{3-x}Yb_xTCAS_2$, x = 1, 2), which are discrete and kinetically stable. Other features include the feasibility of selective synthesis for desired heterotrinuclear complexes,[35] preparation of luminescent materials,[43,44] loaded nanoparticles of contrast reagents for magnetic resonance imaging, and therapeutic agents for neutron capture therapy.[45] Hence, our system has a potential for many applications, such as luminescent materials, imaging probes, and multifunctional agents.

We further extended the UC system to the Tb–Yb–TCAS system, showing luminescence at 486 and 550 nm, assigned to the Tb-centered transitions $^5D_4 \rightarrow {}^7F_5$ and $^7F_6$, respectively, upon Yb excitation (Fig. 4b). The intensity of the Tb-centered luminescence depended on the incident laser power, which exhibited a linear relationship with a slope of 1.8 (Fig. 4c). The slope suggests a two-photon mechanism, such as cooperative energy transfer (Fig. S8b, ESI†). However, the slope's slight deviation from two might be caused by the saturation of excited states of Yb due to the high-power laser, as well as the low efficiency in Yb → Tb energy transfer. These observations are the same as those in the case of the Tb → Yb energy transfer (η = 45%)[33] in $Tb_{3-x}Yb_xTCAS_2$ (x = 1, 2). The intensity of the UC luminescence in the Tb–Yb–TCAS system was weaker and noisier than that of the Er–Yb–TCAS system, which may also be caused by the low Yb → Tb energy transfer efficiency. On the other hand, the $Tb_{3-x}Yb_xTCAS_2$ (x = 0–3) complexes were also stable during NIR laser irradiation (Fig. S9c and d, ESI†).

Our investigation revealed efficient Yb → Er energy transfer in heterotrinuclear cluster complexes ($Er_{3-x}Yb_xTCAS_2$, x = 1, 2), resulting in two-photon UC luminescence in the visible region
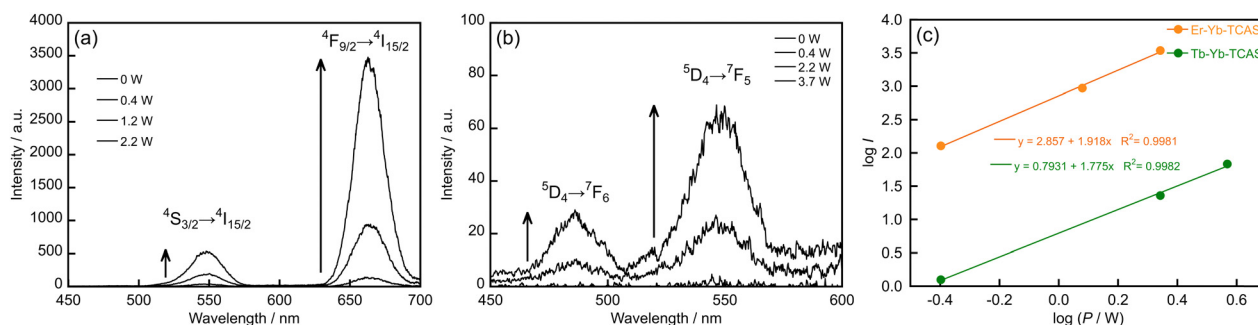

Fig. 4 UC emission spectra of the (a) Er–Yb–TCAS and (b) Tb–Yb–TCAS systems by NIR excitation, and (c) log–log plot of the luminescence intensity (*I*) depending on the NIR laser power (*P*). Er–Yb–TCAS system: [Er] = [Yb] = 1.5 mM, [TCAS] = 2.0 mM, [NH₃] = 0.1 M, pH 10. Tb–Yb–TCAS system: [Tb] = [Yb] = 1.5 mM, [TCAS] = 2.0 mM, [NH₃] = 0.1 M, pH 10, λ_{ex} = 972 nm. (c): λ_{em} = 663 nm for Er–Yb–TCAS system and 550 nm for Tb–Yb–TCAS system.

in aqueous solutions at room temperature. Furthermore, the Tb–Yb–TCAS system exhibited UC luminescence. The arrangement of Ln ions in close proximity to the Ln_3TCAS_2 cluster complex was responsible for the high energy transfer efficiency and UC. The investigation of the applications of these complexes as UC probes and UC photonic materials is currently in progress.

Data availability

The data supporting this article have been included as part of the ESI.†

Conflicts of interest

There are no conflicts to declare.

Notes and references

1 F. Auzel, *Chem. Rev.*, 2004, **104**, 139–173.
2 C. Andraud and O. Maury, *Eur. J. Inorg. Chem.*, 2009, 4357–4371.
3 T. N. Singh-Rachford and F. N. Castellano, *Coord. Chem. Rev.*, 2010, **254**, 2560–2573.
4 L. Aboshyan-Sorgho, M. Cantuel, S. Petoud, A. Hauser and C. Piguet, *Coord. Chem. Rev.*, 2012, **256**, 1644–1663.
5 X. Huang, S. Han, W. Huang and X. Liu, *Chem. Soc. Rev.*, 2013, **42**, 173–201.
6 N. Kimizuka, N. Yanai and M.-A. Morikawa, *Langmuir*, 2016, **32**, 12304–12322.
7 F. Heinemann, J. Karges and G. Gasser, *Acc. Chem. Res.*, 2017, **50**, 2727–2736.
8 W. Ahmad, J. Wang, H. Li, Q. Ouyang, W. Wu and Q. Chen, *Coord. Chem. Rev.*, 2021, 439.
9 F. Lahoz, C. Pérez-Rodríguez, S. E. Hernández, I. R. Martín, V. Lavín and U. R. Rodríguez-Mendoza, *Sol. Energy Mater. Sol. Cells*, 2011, **95**, 1671–1677.
10 E. L. Cates, S. L. Chinnapongse, J. H. Kim and J. H. Kim, *Environ. Sci. Technol.*, 2012, **46**, 12316–12328.
11 J. Zhou, Q. Liu, W. Feng, Y. Sun and F. Li, *Chem. Rev.*, 2014, **115**, 395–465.
12 L. J. Charbonnière, *Dalton Trans.*, 2018, **47**, 8566–8570.
13 B. Golesorkhi, A. Fürstenberg, H. Nozary and C. Piguet, *Chem. Sci.*, 2019, **10**, 6876–6885.
14 A. M. Nonat and L. J. Charbonnière, *Coord. Chem. Rev.*, 2020, **409**, 213192.
15 B. Golesorkhi, H. Nozary, A. Fürstenberg and C. Piguet, *Mater. Horiz.*, 2020, **7**, 1279–1296.
16 A. Nonat, C. F. Chan, T. Liu, C. Platas-Iglesias, Z. Liu, W.-T. Wong, W.-K. Wong, K.-L. Wong and L. J. Charbonnière, *Nat. Commun.*, 2016, **7**, 11978.
17 N. Souri, P. Tian, C. Platas-Iglesias, K.-L. Wong, A. Nonat and L. J. Charbonnière, *J. Am. Chem. Soc.*, 2017, **139**, 1456–1459.
18 A. Nonat, S. Bahamyirou, A. Lecointre, F. Przybilla, Y. Mély, C. Platas-Iglesias, F. Camerel, O. Jeannin and L. J. Charbonnière, *J. Am. Chem. Soc.*, 2019, **141**, 1568–1576.
19 L. K. Soro, C. Charpentier, F. Przybilla, Y. Mély, A. M. Nonat and L. J. Charbonnière, *Chemistry*, 2021, **3**, 1037–1046.
20 L. Aboshyan-Sorgho, C. Besnard, P. Pattison, K. R. Kittilstved, A. Aebischer, J. Claude, G. Bünzli, A. Hauser and C. Piguet, *Angew. Chem., Int. Ed.*, 2011, **50**, 4108–4112.
21 Y. Suffren, D. Zare, S. V. Eliseeva, L. Guénée, H. Nozary, T. Lathion, L. Aboshyan-Sorgho, S. Petoud, A. Hauser and C. Piguet, *J. Phys. Chem. C*, 2013, **117**, 26957–26963.
22 D. Zare, Y. Suffren, L. Guénée, S. V. Eliseeva, H. Nozary, L. Aboshyan-Sorgho, S. Petoud, A. Hauser and C. Piguet, *Dalton Trans.*, 2015, **44**, 2529–2540.
23 Y. Suffren, B. Golesorkhi, D. Zare, L. Guénée, H. Nozary, S. V. Eliseeva, S. Petoud, A. Hauser and C. Piguet, *Inorg. Chem.*, 2016, **55**, 9964–9972.
24 D. Zare, Y. Suffren, H. Nozary, A. Hauser and C. Piguet, *Angew. Chem., Int. Ed.*, 2017, **56**, 14612–14617.
25 B. Golesorkhi, H. Nozary, L. Guénée, A. Fürstenberg and C. Piguet, *Angew. Chem., Int. Ed.*, 2018, **57**, 15172–15176.
26 B. Golesorkhi, I. Taarit, H. Bolvin, H. Nozary, J.-R. Jiménez, C. Besnard, L. Guénée, A. Fürstenberg and C. Piguet, *Dalton Trans.*, 2021, **50**, 7955–7968.
27 B. Golesorkhi, S. naseri, L. Guénée, I. Taarit, F. Alves, H. Nozary and C. Piguet, *J. Am. Chem. Soc.*, 2021, **143**, 15326–15334.
28 R. C. Knighton, L. K. Soro, A. Lecointre, G. Pilet, A. Fateeva, L. Pontille, L. Francés-Soriano, N. Hildebrandt and L. J. Charbonnière, *Chem. Commun.*, 2021, **57**, 53–56.
29 R. C. Knighton, L. K. Soro, L. Francés-Soriano, A. Rodríguez-Rodríguez, G. Pilet, M. Lenertz, C. Platas-Iglesias, N. Hilderbrandt and L. J. Charbonnière, *Angew. Chem., Int. Ed.*, 2022, **61**, e202113114.
30 D. A. Galico, R. Ramdani and M. Murugesu, *Nanoscale*, 2022, **14**, 9675–9680.
31 N. Iki, E. Boros, M. Nakamura, R. Baba and P. Caravan, *Inorg. Chem.*, 2016, **55**, 4000–4005.
32 N. Iki, T. Tanaka, S. Hiro-oka and K. Shinoda, *Eur. J. Inorg. Chem.*, 2016, 5020–5027.
33 N. Iki, in *Calixarenes and Beyond*, ed. P. Neri, J. L. Sessler and M.-X. Wang, Springer International Publishing, Cham, 2016, 13, pp. 335–362.
34 R. Karashimada and N. Iki, *Chem. Commun.*, 2016, **52**, 3139–3142.
35 R. Karashimada, K. Musha and N. Iki, *Bunseki Kagaku*, 2022, **71**, 145–151.
36 N. Morohashi and N. Iki, in *Handbook on the Physics and Chemistry of Rare Earths*, ed. J.-C. G. Bünzli and V. K. Pecharsky, Elsevier, 2022, vol. 62, pp. 1–280.
37 A. Bilyk, J. W. Dunlop, R. O. Fuller, A. K. Hall, J. M. Harrowfield, M. W. Hosseini, G. A. Koutsantonis, I. W. Murray, B. W. Skelton, A. N. Sobolev, R. L. Stamps and A. H. White, *Eur. J. Inorg. Chem.*, 2010, 2127–2152.
38 S. Fischer, B. Fröhlich, K. W. Krämer and J. C. Goldschmidt, *J. Phys. Chem. C*, 2014, **118**, 30106–30114.
39 J. Wang, Y. Jiang, J. Y. Liu, H. B. Xu, Y. X. Zhang, X. Peng, M. Kurmoo, S. W. Ng and M. H. Zeng, *Angew. Chem., Int. Ed.*, 2021, **60**, 22368–22375.
40 F. Artizzu, F. Quochi, L. Marchiò, E. Sessini, M. Saba, A. Serpe, A. Mura, M. L. Mercuri, G. Bongiovanni and P. Deplano, *J. Phys. Chem. Lett.*, 2013, **4**, 3062–3066.
41 F. Artizzu, F. Quochi, L. Marchiò, C. Figus, D. Loche, M. Atzori, V. Sarritzu, A. M. Kaczmarek, R. V. Deun, M. Saba, A. Serpe, A. Mura, M. L. Mercuri, G. Bongiovanni and P. Deplano, *Chem. Mater.*, 2015, **27**, 4082–4092.
42 S. Comby and J.-C. G. Bünzli, in *Handbook on the Physics and Chemistry of Rare Earths*, ed. J. K. A. Gschneidner, J.-C. G. Bünzli and V. K. Pecharsky, Elsevier, 2007, vol. 37, pp. 217–470.
43 N. Shiraishi, R. Karashimada and N. Iki, *Bull. Chem. Soc. Jpn.*, 2019, **92**, 1847–1852.
44 N. Shiraishi, D. Iikura, R. Karashimada and N. Iki, *J. Lumin.*, 2024, **269**, 120521.
45 K. Ohama, M. Komiya, T. Yamatoya, R. Sawamura, R. Karashimada, S. Gao, Y. Ozawa, K. Osada, I. Aoki, T. Nagasaki, M. Suzuki and N. Iki, *Colloids Surf., A*, 2024, **699**, 134579.